molbank

MDPI

Short Note

3-(4-Bromophenyl)-4-{[3-hydroxy-6-(hydroxymethyl)-4-oxo-4*H*-pyran-2-yl](*m*-tolyl)methyl}isoxazol-5(2*H*)-one

Yuliya E. Ryzhkova, Fedor V. Ryzhkov and Michail N. Elinson *

N. D. Zelinsky Institute of Organic Chemistry Russian Academy of Sciences, 47 Leninsky Prospekt, 119991 Moscow, Russia; julia4912@mail.ru (Y.E.R.); ryzhkov.fe@ya.ru (F.V.R.)

* Correspondence: elinson@ioc.ac.ru; Tel.: +7-499-137-3842

Received: 24 April 2020; Accepted: 12 May 2020; Published: 13 May 2020

Abstract: In this communication, the electrochemically induced multicomponent transformation of 3-methylbenzaldehyde, 3-(4-bromophenyl)isoxazol-5(4*H*)-one and kojic acid in *n*-PrOH in an undivided cell in the presence of sodium bromide was carefully investigated to give 3-(4-bromophenyl)-4-{[3-hydroxy-6-(hydroxymethyl)-4-oxo-4*H*-pyran-2-yl](*m*-tolyl)methyl}isoxazol-5(2*H*)-one in good yield. The structure of the new compound was established by means of elemental analysis, mass-, nuclear magnetic resonance and infrared spectroscopy. Furthermore, its structure was determined and confirmed by X-ray analysis. The synthesized compound is a promising compound for different biomedical applications, and, in particular, for the regulation of inflammatory diseases, as shown by docking studies in this research.

Keywords: electrochemistry; 3-methylbenzaldehyde; 3-(4-bromophenyl)isoxazol-5(4*H*)-one; kojic acid; X-ray structure determination; docking studies

1. Introduction

Among different strategies of drug discovery, the identification and application of "privileged structures or scaffolds" have gained special attention in the last decades [1,2]. These privileged scaffolds are constructed from a rigid heterocyclic system, which determine the orientation type of different functional substituents in order to be recognized by a target molecule [3].

Kojic acid's derivatives show antibacterial [4], antidiabetic [5], anticancer [6] activities and inhibit human neutrophil's elastase [7]. Isoxazol-5(4*H*)-one derivatives have demonstrated antagonistic anti-androgen activity on human prostate tumor LNCaP cells [8], and they are also known as antitumor [9], anti-inflammatory [10], antiviral [11], and analgesic [12] agents.

Thus, diverse therapeutic activities of kojic acid and isoxazol-5(4*H*)-one derivatives explain the interest in the combination of both of these fragments.

Herein, we report the electrochemically induced synthesis of the previously unknown 3-(4-bromophenyl)-4-{[3-hydroxy-6-(hydroxymethyl)-4-oxo-4*H*-pyran-2-yl](*m*-tolyl)methyl}isoxazol-5(2*H*)-one and present the study of its structure and pharmacological activity.

2. Results and Discussion

2.1. Research of Electrochemically Induced Multicomponent Synthesis of 3-(4-Bromophenyl)-4-{[3-hydroxy-6-(hydroxymethyl)-4-oxo-4H-pyran-2-yl](m-tolyl)methyl}isoxazol-5(2H)-one **4**

MCRs (multicomponent reactions) were considered as an important instrument to perform an "ideal synthesis" [13], however, electrocatalytic and electrochemically induced multicomponent

reactions bring additional value to green synthesis [14]. Moreover, the multicomponent reaction strategy is closely related with the PASE (pot, atom, step economic) strategy [15], which postulates pot, atom and step economy.

We have already carried out some electrochemically induced multicomponent transformations of carbonyl compounds and different C-H acids [16,17].

Now, we wish to report our results on the selective and efficient 'one-pot' electrochemically induced transformation of 3-methylbenzaldehyde **1**, 3-(4-bromophenyl)isoxazol-5(4*H*)-one **2** and kojic acid **3** into the previously unknown 3-(4-bromophenyl)-4-{[3-hydroxy-6-(hydroxymethyl)-4-oxo-4*H*-pyran-2-yl](*m*-tolyl)methyl}isoxazol-5(2*H*)-one **4** in *n*-PrOH at 97 °C in the undivided cell in the presence of sodium bromide under constant current density conditions, as shown in Scheme 1. The catalytic amount of electricity that passed through the reaction mixture was 0.3 F/mol. A graphite anode, an iron cathode and constant current density of 5 mA/cm^2 (I = 25 mA, electrodes square 5 cm^2) were used for the process.

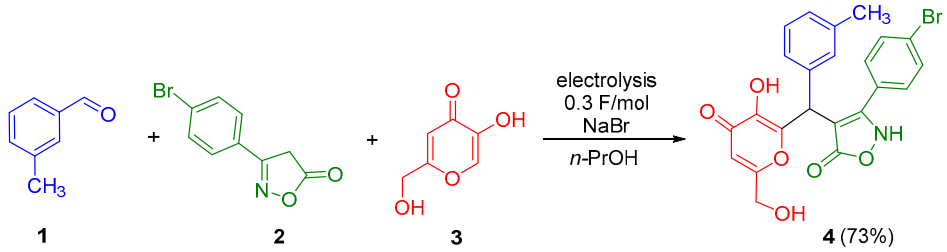

Scheme 1. Synthesis of 3-(4-bromophenyl)-4-{[3-hydroxy-6-(hydroxymethyl)-4-oxo-4*H*-pyran-2-yl]-(*m*-tolyl)methyl}isoxazol-5(2*H*)-one **4**.

Compound **4** was synthesized in 73% substance yield with 243% current efficiency.

Taken into consideration the results on electrocatalytic assembling of carbonyl compounds and C-H acids [16], the following mechanism for the multicomponent transformation of 3-methylbenzaldehyde **1**, 3-(4-bromophenyl)isoxazol-5(4*H*)-one **2** and kojic acid **3** into 3-(4-bromophenyl)-4-{[3-hydroxy-6-(hydroxymethyl)-4-oxo-4*H*-pyran-2-yl](*m*-tolyl)methyl}isoxa-zol-5(2*H*)-one **4** was proposed, as shown in Scheme 2.

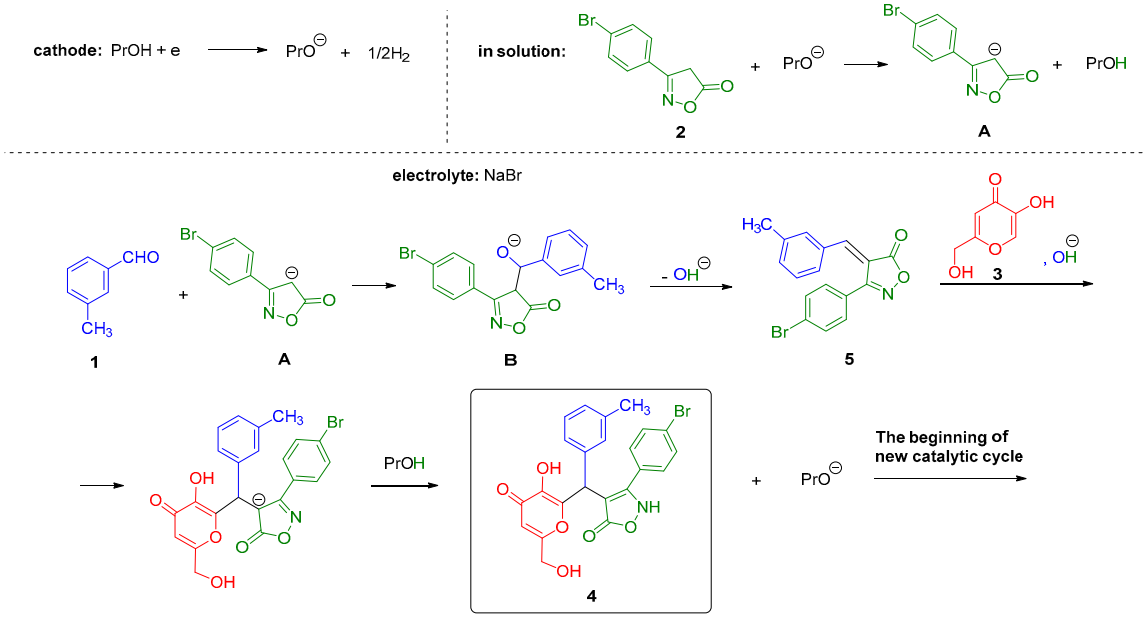

Scheme 2. Mechanism of electrocatalytic multicomponent transformation.

The first step of the electrochemically induced process of the deprotonation of *n*-propanol at the cathode leads to the formation of a *n*-propoxide anion with a release of hydrogen gas [16]. Then, the *n*-propoxide anion interaction with 3-(4-bromophenyl)isoxazol-5(4*H*)-one **2** provides the 3-(4-bromophenyl)isoxazol-5(4*H*)-one anion **A** formation. The following process is Knoevenagel condensation of the anion **A** and 3-methylbenzaldehyde **1** with the elimination of a hydroxide anion and the formation of adduct **5** [18]. The subsequent hydroxide-anion promoted Michael addition of kojic acid **3** to the electron deficient Knoevenagel adduct **5**, which leads to the end compound **4** in the electrocatalytic chain process, namely, 3-(4-bromophenyl)-4-{[3-hydroxy-6-(hydroxymethyl)-4-oxo-4*H*-pyran-2-yl](*m*-tolyl)methyl}isoxazol-5(2*H*)-one **4** with the regeneration of the *n*-propoxide anion as the last step of the catalytic cycle. The catalytic chain process continues by the interaction of the *n*-propoxide anion with the next molecule of 3-(4-bromophenyl)isoxazol-5(4*H*)-one **2**.

2.2. X-ray Diffraction Data

The structure of compound **4** is confirmed by X-ray crystallography, as shown in Figure 1. Thermal ellipsoids correspond to 50% probability. The crystal is a racemate, containing equal numbers of both enantiomers.

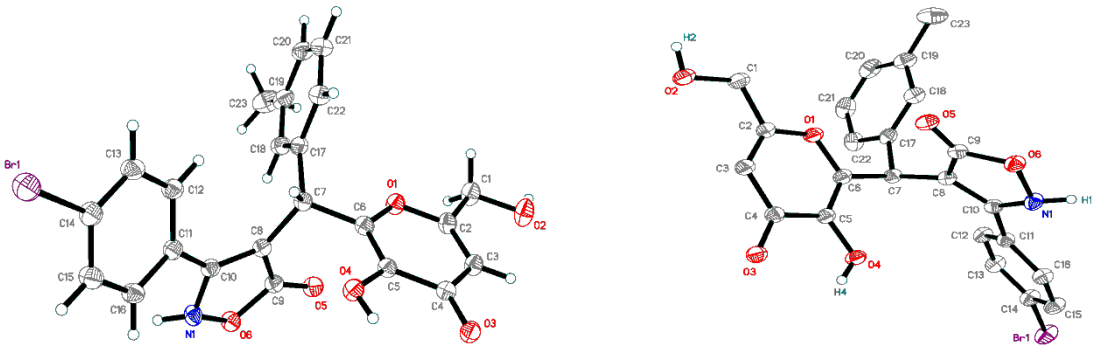

Figure 1. The structure of compound **4** (XRD—X-ray Diffraction). The crystal is a racemate, which contains enantiomers (**a**,**b**).

The Cambridge Crystallographic Data Centre (CCDC) 1,996,890 contains the supplementary crystallographic data for this paper, which can be obtained from The Cambridge Crystallographic Data Centre via http://www.ccdc.cam.ac.uk.

Crystal data for $C_{23}H_{18}BrNO_6$ (**4**) (M = 484.29 g/mol): monoclinic, space group $P2_1/n$, a = 9.4765(3) Å, b = 9.2067(3) Å, c = 24.1253(7) Å, β = 92.1209(7)°, V = 2103.42(11) $Å^3$, Z = 4, T = 100(2) K, μ(CuKα) = 1.995 mm^{-1}, Dcalc = 1.529 g/cm^3, 82,080 reflections measured (2.340° ≤ Θ ≤ 31.510°), 7000 unique (Rint = 0.0565) which were used in all calculations. The final R1 was 0.0400 (I > 2σ(I)) and wR2 was 0.0893 (all data).

2.3. Docking Studies

During molecular docking studies, the binding modes of protein-ligand complexes were investigated using Lead Finder software (BioMolTech Corp) [19]. Lead Finder uses three specialized high accuracy scoring functions for binding energy prediction, rank-ordering of compounds in virtual screening experiments (with ordering most active to least active compound), and energy-ranking of docked ligand poses. This approach is semiempirical, molecular and mechanically functional and produces high accuracy predictions confirmed by numerous experiments [20].

The human C5a receptor was chosen for the study (PDB code: 6C1R) as it modulates inflammatory responses. It also modulates obesity, development and cancers [21–23]. The new synthesized compound **4** was subjected to the docking procedure.

Compound **4** showed good binding affinities of −8.63 kcal × mol^{-1} and a good virtual screening score of −10.25. Pose ranking also revealed good results. The best mode was ranked with a score of −7.71. However, affinity calculated for **W54011** (known C5a receptor antagonist) [24] was −8.68 kcal × mol^{-1} and the screening score was −9.70 for the best binding mode (−7.49).

Figure 2 shows that compound **4** formed hydrogen interactions between the kojic fragment and THR303, ILE306 residues, as well as between the isoxazol fragment and CYS307, ALA218, ALA214 residues. One CH–π interaction was designed between 4-bromophenyl fragment and ALA214 residue.

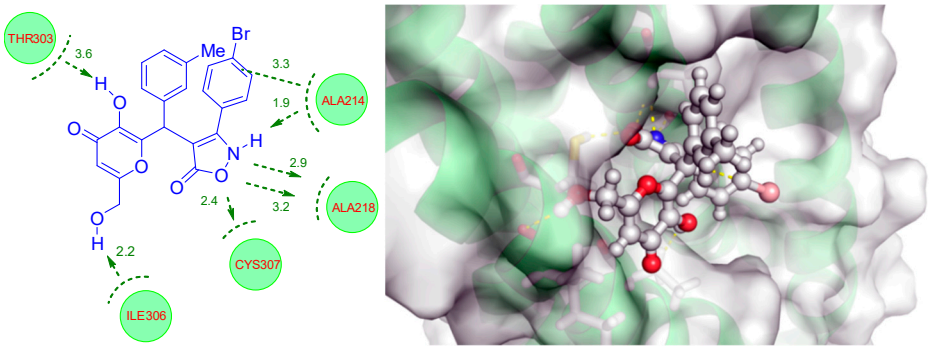

Figure 2. Interaction of compound **4** with the amino acids of C5a (arrows show the distances in angstrom between atoms).

To sum up, compound **4** showed good results according to the LeadFinder virtual screening scoring function, pose ranking and calculated binding energy. Taking into consideration the above results, one can conclude that compound **4** is comparable to (or better than) the known C5a receptor antagonist—**W54011**.

3. Materials and Methods

3.1. General Methods

The solvents and reagents were purchased from commercial sources and used as received. 3-(4-Bromophenyl)isoxazol-5(4*H*)-one **2** was obtained in two steps from 4′-bromoacetophenone according to the literature [25,26].

All melting points were measured with Gallenkamp melting-point apparatus (London, UK) and were uncorrected. ^{1}H and ^{13}C NMR spectra were recorded in DMSO-d_6 with a Bruker Avance II 300 spectrometer (Billerica, MA, USA) at ambient temperature. OH and NH signals were exchanged with D_2O (it is present as an impurity in DMSO-d_6). Chemical shift values are relative to Me_4Si. IR spectrum was recorded with a Bruker ALPHA-T FT-IR spectrometer (Billerica, MA, USA) in KBr pellet. MS spectrum (EI = 70 eV) was obtained directly with a Kratos MS-30 spectrometer (Manchester, UK). For elemental analysis, 2400 Elemental Analyzer (Perkin Elmer Inc., Waltham, MA, USA) was used.

X-ray diffraction data were collected at 100K on a Bruker Quest D8 diffractometer (Billerica, MA, USA) equipped with a Photon-III area-detector (graphite monochromator, shutterless φ- and ω-scan technique), using Mo K_α-radiation (0.71073 Å). The intensity data were integrated by the SAINT program (version 8.38A) [27] and were corrected for absorption and decay using SADABS [28]. The structure was solved by direct methods using SHELXT [29] and refined on F^2 using SHELXL-2018 [30]. All nonhydrogen atoms were refined with individual anisotropic displacement parameters. Locations of hydroxy and amino H-atoms (H1, H2 and H4) were found from the electron density-difference map. The O-H distances were restrained to be 0.84(2) Å. These hydrogen atoms were refined with individual isotropic displacement parameters. All other hydrogen atoms were placed in ideally calculated positions and refined as riding atoms with relative isotropic displacement parameters. The SHELXTL program suite [27] was used for molecular graphics.

For docking simulation, Lead Finder (version 1.1.16.) by BioMolTech Corp. (Toronto, Ontario, Canada) [19] was used. The default program settings were used for estimation of binding affinity, virtual screening score and rank score. The human C5a receptor was retrieved from the RCSB protein bank (PDB code: 6C1R) [31]. W54011 was selected as the reference compound as a C5a antagonist [24]. The buildmodel tool in Lead Finder was used to treat 6C1R and W54011 before docking studies. Prior to docking studies, the 3D-structure of compound **4** was optimized and hydrogen atoms were set explicitly. The modes, rank scores, binding affinities and virtual screening scores are presented in Table S8 (see Supplementary Materials). Analysis of the protein–ligand interaction was accomplished with PyMOL Molecular Graphics System software (version 2.3.5) by Shrödinger, Inc. (New York, NY, USA).

3.2. Electrochemically Induced Multicomponent Synthesis of 3-(4-Bromophenyl)-4-{[3-hydroxy-6-(hydroxymethyl)-4-oxo-4H-pyran-2-yl](m-tolyl)methyl}isoxazol-5(2H)-one **4**

A solution of 3-methylbenzaldehyde **1** (0.6 g, 5 mmol), 3-(4-bromophenyl)isoxazol-5(4*H*)-one **2** (1.2 g, 5 mmol), kojic acid **3** (0.71 g, 5 mmol) and sodium bromide (0.1 g, 1 mmol) in *n*-propanol (20 mL) was electrolyzed in an undivided cell equipped with a magnetic stirrer, a graphite anode and an iron cathode at 97 °C under a constant current density of 5 mA/cm^2 (I = 25 mA, electrodes square 5 cm^2) until the catalytic quantity of 0.3 F/mol of electricity passed. After the electrolysis was finished, the reaction mixture was concentrated to one fifth of its initial volume (*ca.* 4 mL) and chilled to 0 °C to crystallize the solid compound **4**, which was then filtered out, twice rinsed with an ice-cold ethanol/water solution (3:1, 4 mL), and dried under reduced pressure.

*3-(4-Bromophenyl)-4-{[3-hydroxy-6-(hydroxymethyl)-4-oxo-4H-pyran-2-yl](3-metylphenyl)methyl}isoxazol-5(2H)-one (**4**).* White solid; Yield 73% (1.77 g); mp = 224–225 °C; FT-IR (KBr): 3423 (NH), 3253 (NH), 3031 (OH), 2715 (C-H alkyl), 1700 (C=O), 1650 (C=O), 1605 (Ar C=C), 1548 (Ar C=C), 1478 (C-H alkyl), 1233 (C-O amide) cm^{-1}; ^{1}H NMR (300 MHz, DMSO-d_6): δ 2.20 (s, 3H, CH_3), 4.03 (d, ^2J = 16.4 Hz, 1H, CH_2), 4.08 (d, ^2J = 16.4 Hz, 1H, CH_2), 5.44 (s, 1H, CH), 6.27 (s, 1H, CH), 6.88–6.98 (m, 2H, 2 CH Ar), 7.00 (d, ^3J = 7.4 Hz, 1H, CH Ar), 7.13 (t, ^3J = 7.4 Hz, 1H, CH Ar), 7.27 (d, ^3J = 8.2 Hz, 2H, 2 CH Ar), 7.61 (d, ^3J = 8.2 Hz, 2H, 2 CH Ar) ppm; ^{13}C NMR (75 MHz, DMSO-d_6): δ 21.1 (CH_3), 37.6 (CH aliph.), 59.2 (CH_2), 95.1 (br s, C-CO-O), 108.9 (CH-C=O), 124.3 (C-Br), 125.1 (CH Ar), 126.8 (HN-C-C Ar), 127.6 (CH Ar), 128.4 (CH Ar), 128.6 (CH Ar), 130.1 (2C, 2 CH Ar), 131.7 (2C, 2 CH-C-Br), 137.6 (C-CH_3), 137.9 (CH-C Ar), 141.6 (C-OH), 148.5 (O-C=C-OH), 162.1 (O-NH-C), 167.4 (C-CH_2-OH), 170.9 (O-C=O), 173.4 (HO-C-C=O) ppm; MS (*m/z*, relative intensity %): 342 [^{81}Br, M − $C_6H_6O_4$ − H]$^+$ (1), 340 [^{79}Br, M − $C_6H_6O_4$ − H]$^+$ (1), 285 (2), 246 (41), 245 [M − $C_9H_5BrNO_2$]$^+$ (100), 182 (54), 171 (57), 115 (99), 102 (91), 75 (72), 39 (60); Anal. calcd for $C_{23}H_{18}BrNO_6$: C, 57.04; H, 3.75; Br, 16.50; N, 2.89%; found: C, 56.91; H, 3.63; Br, 16.40; N, 2.82%.

4. Conclusions

The title compound, 3-(4-bromophenyl)-4-{[3-hydroxy-6-(hydroxymethyl)-4-oxo-4*H*-pyran-2-yl](*m*-tolyl)methyl}isoxazol-5(2*H*)-one **4**, was synthesized in good yield using the facile and efficient electrocatalytic approach with simple equipment and available starting compounds. The compound **4** was characterized by spectroscopic methods (NMR, IR, MS-EI) and elemental analysis. Its crystal structure was determined and confirmed by X-ray analysis. According to docking studies with Lead Finder software, the synthesized compound showed good results in virtual screening scoring, pose ranking and calculated binding energy to C5a receptor. When compared with **W54011** (known C5a receptor antagonist, regulates inflammatory), compound **4** showed better results in the current study.

Supplementary Materials: The following are available online, Compound **4** spectra: ^{1}H NMR (Figure S1); ^{13}C NMR (Figure S2); IR (Figure S3); MS (EI) (Figure S4); Crystal data and structure refinement for **4** (Table S1); Atomic coordinates (x 10^4) and equivalent isotropic displacement parameters (Å^2 x 10^3) for **4** (Table S2); Bond lengths [Å] and angles [°] for **4** (Table S3); Anisotropic displacement parameters (Å^2 x 10^3) for **4** (Table S4); Hydrogen coordinates (× 10^4) and isotropic displacement parameters (Å^2 × 10^3) for **4** (Table S5); Torsion angles [°] for **4**

(Table S6); Hydrogen bonds for **4** [Å and °] (Table S7); The results of docking studies (the optimal modes are highlighted in bold font) (Table S8).

Author Contributions: Y.E.R.—synthesis, spectroscopic analysis, writing the manuscript; F.V.R.—docking studies, writing the manuscript; M.N.E.—conceptualization, supervision, writing the manuscript. The authors read and approved the final manuscript. All authors have read and agreed to the published version of the manuscript.

Funding: The reported study was funded by RFBR, project number 19-29-08013.

Acknowledgments: Crystal structure determination was performed in the Department of Structural Studies of Zelinsky Institute of Organic Chemistry, Moscow.

Conflicts of Interest: The authors declare no conflict of interest.

References

1. Schneider, P.; Schneider, G. A Computational Method for Unveiling the Target Promiscuity of Pharmacologically Active Compounds. *Angew. Chem. Int. Ed.* **2017**, *56*, 7971–7994. [CrossRef]
2. Patchett, A.A.; Nargund, R.P. Chapter 26. Privileged structures. *Ann. Rep. Med. Chem.* **2000**, *35*, 289–298. [CrossRef]
3. Poupaert, J.; Carato, P.; Colacino, E.; Yous, S. 2(3*H*)-Benzoxazolone and bioisosters as "privileged scaffold" in the design of pharmacological probes. *Curr. Med. Chem.* **2005**, *12*, 877–885. [CrossRef] [PubMed]
4. Reddy, B.V.S.; Reddy, M.R.; Madan, C.; Kumar, K.P.; Rao, M.S. Indium(III) chloride catalyzed three-component coupling reaction: A novel synthesis of 2-substituted aryl(indolyl)kojic acid derivatives as potent antifungal and antibacterial agents. *Bioorg. Med. Chem. Lett.* **2010**, *20*, 7507–7511. [CrossRef]
5. Sharma, D.K.; Pandey, J.; Tamrakar, A.K.; Mukherjee, D. Synthesis of heteroaryl/aryl kojic acid conjugates as stimulators of glucose uptake by GLUT4 translocation. *Eur. J. Med. Chem.* **2014**, *85*, 727–736. [CrossRef]
6. Nayak, D.; Katoch, A.; Sharma, D.; Faheem, M.M.; Chakraborty, S.; Sahu, P.K.; Chikan, N.A.; Amin, H.; Gupta, A.P.; Gandhi, S.G.; et al. Indolylkojyl methane analogue IKM5 potentially inhibits invasion of breast cancer cells via attenuation of GRP78. *Breast Cancer Res. Treat.* **2019**, *177*, 307–323. [CrossRef]
7. Lucas, S.D.; Gonçalves, L.M.; Carvalho, L.A.R.; Correia, H.F.; Da Costa, E.M.R.; Guedes, R.A.; Moreira, R.; Guedes, R.C. Optimization of O_3-Acyl Kojic Acid Derivatives as Potent and Selective Human Neutrophil Elastase Inhibitors. *J. Med. Chem.* **2013**, *56*, 9802–9806. [CrossRef]
8. Ishioka, T.; Tanatani, A.; Nagasawa, K.; Hashimoto, Y. Anti-androgens with full antagonistic activity toward human prostate tumor LNCaP cells with mutated androgen receptor. *Bioorg. Med. Chem. Lett.* **2003**, *13*, 2655–2658. [CrossRef]
9. Patrizia, D.; Carbone, A.; Barraja, P.; Kelter, G.; Fiebig, H.H.; Cirrincione, G. Synthesis and antitumor activity of 2,5-bis(3′-indolyl)-furans and 3,5-bis(3′-indolyl)-isoxazoles, nortopsentin analogues. *Bioorg. Med. Chem.* **2010**, *18*, 4524–4529. [CrossRef]
10. Karabasanagouda, T.; Adhikari, A.V.; Girisha, M. Synthesis of some new pyrazolines and isoxazoles carrying 4-methylthiophenyl moiety as potential analgesic and anti-inflammatory agents. *Indian J. Chem.* **2009**, *48B*, 430–437.
11. Lee, Y.S.; Park, S.M.; Kim, B.H. Synthesis of 5-isoxazol-5-yl-2′-deoxyuridines exhibiting antiviral activity against HSV and several RNA viruses. *Bioorg. Med. Chem. Lett.* **2009**, *19*, 1126–1133. [CrossRef] [PubMed]
12. Kano, H.; Adachi, I.; Kido, R.; Hirose, K. Isoxazoles. XVIII. Synthesis and Pharmacological Properties of 5-Aminoalkyl- and 3-Aminoalkylisoxazoles and Related Derivatives. *J. Med. Chem.* **1967**, *10*, 411–418. [CrossRef]
13. Gu, Y. Multicomponent reactions in unconventional solvents: State of the art. *Green Chem.* **2012**, *14*, 2091–2128. [CrossRef]
14. Kreysa, G.; Ota, K.; Savinell, R.F. *Encyclopedia of Applied Electrochemistry*; Springer: New York, NY, USA, 2014.
15. Zang, W.; Yi, W.-B. *Pot, Atom and Step Economy (PASE) Synthesis*; Springer International Publishing: Cham, Switzerland, 2019; pp. 1–4.
16. Elinson, M.N.; Dorofeev, A.S.; Nasybullin, R.F.; Fedukovich, S.K.; Nikihin, G.I. Electrocatalytic tandem Knoevenagel–Michael reaction of 3-methyl-2-pyrazolin-5-ones, aryl aldehydes and cyano-functionalized C–H acids: Facile and convenient multicomponent way to substituted 3-(5-hydroxy-3-methylpyrazol-4-yl)-3-arylpropionitriles. *Electrochim. Acta* **2008**, *53*, 5033–5038. [CrossRef]

17. Elinson, M.N.; Nasybullin, R.F.; Nikihin, G.I. Electrocatalytic Fast and Efficient Multicomponent Approach to Medicinally Relevant (2-Amino-4*H*-chromen-4-yl)phosphonate Scaffold. *Heteroatom. Chem.* **2013**, *24*, 398–403. [CrossRef]
18. Patai, S.; Israeli, Y. The kinetics and mechanisms of carbonyl–methylene condensations. Part VII. The reaction of malononitrile with aromatic aldehydes in ethanol. *J. Chem. Soc.* **1960**, 2025–2030. [CrossRef]
19. LeadFinder, Biomoltech, Inc. Available online: http://www.biomoltech.com/ (accessed on 22 April 2020).
20. Stroganov, O.V.; Novikov, F.N.; Stroylov, V.S.; Kulkov, V.; Chilov, G.G. Lead Finder: An Approach To Improve Accuracy of Protein−Ligand Docking, Binding Energy Estimation, and Virtual Screening. *J. Chem. Inf. Model.* **2008**, *48*, 2371–2385. [CrossRef]
21. Brennan, F.H.; Gordon, R.; Lao, H.W.; Biggins, P.J.; Taylor, S.M.; Franklin, R.J.; Woodruff, T.M.; Ruitenberg, M.J. The Complement Receptor C5aR Controls Acute Inflammation and Astrogliosis following Spinal Cord Injury. *J. Neurosci. Res.* **2015**, *35*, 6517–6531. [CrossRef]
22. Lim, J.; Iyer, A.; Suen, J.Y.; Seow, V.; Reid, R.C.; Brown, L.; Fairlie, D.P. C5aR and C3aR antagonists each inhibit diet-induced obesity, metabolic dysfunction, and adipocyte and macrophage signaling. *FASEB J.* **2013**, *27*, 822–831. [CrossRef]
23. Markiewski, M.M.; DeAngelis, R.A.; Benencia, F.; Ricklin-Lichtsteiner, S.K.; Koutoulaki, A.; Gerard, C.; Coukos, G.; Lambris, J.D. Modulation of the antitumor immune response by complement. *Nat. Immunol.* **2008**, *9*, 1225–1235. [CrossRef]
24. Seow, V.; Lim, J.; Cotterell, A.; Yau, M.-K.; Xu, W.; Lohman, R.J.; Kok, W.M.; Stoermer, M.J.; Sweet, M.J.; Reid, R.C.; et al. Receptor residence time trumps drug-likeness and oral bioavailability in determining efficacy of complement C5a antagonists. *Sci. Rep.* **2016**, *6*, 24575. [CrossRef] [PubMed]
25. Ko, T.Y.; Youn, S.W. Cooperative Indium(III)/Silver(I) System for Oxidative Coupling/Annulation of 1,3-Dicarbonyls and Styrenes: Construction of Five-Membered Heterocycles. *Adv. Synth. Catal.* **2016**, *358*, 1934–1941. [CrossRef]
26. Griesbeck, A.G.; Franke, M.; Neudörfl, J.; Kotaka, H. Photocycloaddition of aromatic and aliphatic aldehydes to isoxazoles: Cycloaddition reactivity and stability studies. *Beilstein J. Org. Chem.* **2011**, *7*, 127–134. [CrossRef] [PubMed]
27. *Bruker. APEX-III*; Bruker AXS Inc.: Madison, WI, USA, 2018.
28. Krause, L.; Herbst-Irmer, R.; Sheldrick, G.M.; Stalke, D. Comparison of silver and molybdenum microfocus X-ray sources for single-crystal structure determination. *J. Appl. Cryst.* **2015**, *48*, 3–10. [CrossRef] [PubMed]
29. Sheldrick, G.M. SHELXT - Integrated space-group and crystal-structure determination. *Acta Cryst.* **2015**, *A71*, 3–8. [CrossRef] [PubMed]
30. Sheldrick, G.M. Crystal structure refinement with SHELXL. *Acta Cryst.* **2015**, *C71*, 3–8. [CrossRef]
31. Liu, H.; Kim, H.R.; Deepak, R.N.V.K.; Wang, L.; Chung, K.Y.; Fan, H.; Wei, Z.; Zhang, C. Orthosteric and allosteric action of the C5a receptor antagonists. *Nat. Struct. Mol. Biol.* **2018**, *25*, 472–481. [CrossRef]